2014-01-01

Equations of State in a Strongly Interacting Relativistic System

Jason Paul Keith
University of Texas at El Paso, 472853@gmail.com

EQUATIONS OF STATE IN A STRONGLY INTERACTING RELATIVISTIC SYSTEM

Jason P. Keith

Department of Physics

APPROVED:

Efrain Ferrer, Chair, Ph.D.

Vivian de la Incera, Ph.D.

Piotr Wojciechowski, Ph.D.

Juan Noveron, Ph.D.

Bess Sirmon-Taylor, Ph.D.

Interim Dean of the Graduate School

EQUATIONS OF STATE IN A STRONGLY INTERACTING RELATIVISTIC SYSTEM

by

Jason P. Keith

THESIS

Presented to the Faculty of the Graduate School of

The University of Texas at El Paso

in Partial Fulfillment

of the Requirements

for the Degree of

MASTER OF SCIENCE

Department of Physics

THE UNIVERSITY OF TEXAS AT EL PASO

August 2014

Acknowledgements

This work was conducted under the advisement of Dr. E.J. Ferrer at the University of Texas at El Paso, and has been supported by the UTEP-COURI-2011 grant and DOE Nuclear Theory grant de-sc0002179. Special thanks to Israel Portillo for advice on computational methods, Vivian de la Incera, and the rest of the high-energy theory group.

Abstract

It has long been understood that the ground state of a superdense quark system, a Fermi liquid of weakly interacting quarks, is unstable with respect to the formation of diquark condensates. This nonperturbative phenomenon is essentially equivalent to the Cooper instability of conventional BCS superconductivity. As the quark pairs have nonzero color charge, this kind of superconductivity breaks the SU(3) color gauge symmetry, thus the phenomenon is called color superconductivity. However, not much is known about the behavior of quark systems at moderate densities between the formation of baryons and asymptotic freedom. Strong theoretical and experimental evidence suggests that there will be a smooth crossover between the two, during which the color superconducting properties of the quark system will undergo a shift between dynamics of a Bose-Einstein condensate (BEC) and weakly bound diquark pairs governed by BCS theory. Chromomagnetic instabilities exist for the densities in question and it is unclear what phase will resolve them. Therefore, there are many different proposed models accounting for several possible phases in need of thorough investigation. The analysis of two simple models that exhibit the crossover between a BCS state and a Bose-Einstein Condensate (BEC), as well as the evolution of the corresponding equation of state through the crossover, are the topics of this thesis.

Table of Contents

List of Figures

Chapter 1

Introduction

The strong nuclear interaction is one of the four fundamental interactions of nature. Governed by quantum chromodynamics (QCD) it provides a description of how nucleons (protons and neutrons) stay bound together in a nucleus via their constituent particles, known as quarks, which couple with the strong force. Quarks are fundamental particles, classified as *fermions*, spin-1/2 particles, which are predicted to exist by the *Standard Model* of particle physics. Quarks couple to the strong nuclear interaction which, unlike the electromagnetic interaction, has three different charges called *colors*. Quarks also come in several different *species*. The three species relevant to the current topic are *up* (u), *down* (d), and *strange* (s), this introduces a new degree of freedom referred to as *flavor*. Although individual quarks have never been observed in a lab, one possible explanation for this lack of observational evidence could be attributed to the nature of the strong interaction whose coupling constant, or strength of the interaction, increases as distance increases between the interacting particles, meaning that separating them requires increasing amounts of energy. On the other hand, at very small distance their interaction becomes negligibly small. That is, very energetic quarks that can be very close do not interact. This is what is called the *asymptotic freedom* of the strong interaction. It is thought that under extreme temperature and negligible pressures, quarks may experience *deconfinement* and overcome the strong attraction to become unbound free particles. Interestingly, that is not the only way in which quarks might act as free particles considering that if, rather than providing enough energy to liberate them, one were to compress the hadrons decreasing the average separation of their consituent quarks, this would decrease the coupling strength to arbitrarily low values. The boundaries of previously distinct hadrons then overlap leaving only a dense fermion gas of approximately freely

moving fermions in asymptotic freedom.

Asymptotic freedom was first described in 1973 by David Gross, Frank Wilczek, and David Politzer [1] for which they shared a Nobel prize in 2004. When asymptotic freedom occurs the quarks may be thought of approximately as free particles.

The immense pressure and relatively low temperatures that can be found within the cores of dense neutron stars might provide adequate conditions for asymptotic freedom to manifest. Because fermions are subject to the *Pauli exclusion principle* (discussed in section 2.3) they populate all energy states up to the Fermi-surface. The physics of a weakly interacting system such as this, is already well described in the context of superconductivity of electrons within a framework known as *BCS theory* (named after its creators Bardeen, Cooper, and Schreifer), in which the electrons experience an attractive potential due to phonon interactions allowing them to form bound states of two electrons with opposite spins called *Cooper pairs*. This framework can readily be applied to the context of cold asymptotically free quarks as well since the Cooper instability described by the theory applies to any fermionic system with an attractive interaction at sufficiently low temperature. These conditions suit color superconductivity well due to quark interactions in QCD possessing attractive channels. The theory resolves the instability with the creation of Cooper pairs, two quarks with opposite momentum and spin bound together by their weak attraction, resulting in a gap for the energy required to create a particle at the Fermi surface such that no excitation energies exist with vanishing free energy. The formed state of matter is known as a *color superconductor*, where the term *color* comes from the fact that the ground state is now charged with respect to the color charge.

In temperature versus chemical potential plane of the QCD phase diagram the region of asymptotically large μ and zero T is well understood in the context of weakly coupled QCD, in which all the quarks are paired in diquarks in the energetically favored Color-Flavor-Locked (CFL) superconducting phase. The CFL phase is characterized by a zero spin diquark condensate which is antisymmetric in both color and flavor. Besides looking for signatures of color superconductivity in neutron stars there are experiments planned which

could possibly probe color superconductivity in the future at locations such as the Facility for Antiproton and Ion Research (FAIR) at GSI, the Nuclotron-Ion Collider Facility (NICA) at JINR, the Japan Proton Accelerator Research Complex (JPARK) at JAERI, Brookhaven National Lab (BNL) at RHIC, and CERN at the LHC [25].

Chiral models of QCD, which take the limit as the fermion mass tends to zero, predict critical points in the QCD phase diagram (shown in Section 2.4) implying that beneath the relevant critical point might lie a region in which hadronic matter is capable of smoothly transitioning into a color superconductor rather than undergoing a phase transition. This smooth transition is called a *crossover*.

It is thought that in smoothly fine tuning the diquark coupling strength, which might be thought of as increasing as the radial distance decreases to the center of the neutron star, the Fermi gas gives rise to a regime where the fermions are bound into states of quark pairs with all combinations of colors and flavors in the so called Color-Flavor-Locked (CFL) phase [11]. These pairs would then comprise of a *composite boson*, which is no longer subject to the Pauli exclusion principle, which at such low temperatures would correspond to a *Bose-Einstein-condensate* (BEC) and might still retain its color superconducting properties due to the fact that the ground state is now color charged.

Decreasing the density it was found that there exists chromomagnetic instabilities, which are exhibited as a consequence of mismatched Fermi momenta of different quarks produced by the strange quark mass m_s together with the constraints imposed by electric and color neutralities. Due to such instabilities it is unclear what phase is most stable for a color superconductor at intermediate densities as those between hadronic matter and color superconducting CFL phase at high density. Therefore, exploratory work is being done in this area to remove the chromomagnetic instabilities [26]. Several interesting models have been proposed, such as a CFL-phase modified to include a kaon condensate [27], a LOFF phase on which the quarks pair with nonzero total momentum [28], and an inhomogeneous gluon condensate [29]. To obtain deeper insight into the nature of the unknown stable phase is the motivation of our research.

1.1 Objectives of Thesis

The objective of this thesis is to present an overview of the physics and recent developments surrounding the smooth crossover, described above, in the dynamics of color superconductors between BCS and BEC descriptions. We will consider two simplified toy models to investigate the BCS-BEC crossover and analyze its impact in the systems' equations of state (EoS). The results and conclusions presented here are, therefore, not definitive within the overall framework of QCD but serve to provide deeper insight toward that goal. The Lagrangians of each respective model will allow calculation of thermodynamic potentials, which will be set to zero temperature as is the limit for the states of matter, which are most interesting for astrophysical applications. One of the models in question will contain both bosonic and fermionic degrees of freedom, which are treated as separate degrees of freedom, and a second model describing a simple four fermion interaction in which only fermionic degrees of freedom exist, but its bosonic behavior is realized through the formation of diquarks. We then can take the difermion coupling strength to act as a crossover parameter to drive the system between higher and lower density regions, effectively moving between the domains of BCS and BEC dynamics smoothly. In doing this, we will observe similar implications for the stability of the star within both models.

The thesis will be organized as follows: Chapter 2 will serve to introduce the necessary formalism and the theoretical background used in later chapters. In Chapter 3 we introduce a simple model for the crossover in which the system is taken to possess fermionic and bosonic degrees of freedom. Chapter 4 then presents a second model with only fermionic degrees of freedom, where the crossover occurs via a shift between the nature of the system quasiparticles at some critical value of the diquark attractive coupling. Finally, in Chapter 5 we conclude with a general discussion of the obtained results, a comparison between the two models, and an outlook of needed future investigagions.

Chapter 2

Theoretical Background

2.1 Equations of State and Thermodynamic Potentials

Equations of state are relations between dynamical *state variables* that can include any of the following: temperature T, entropy S, pressure p, volume V, chemical potential μ, and particle number N. The last two can be defined for each species of particle in the system.

One is able to find relations between these variables by the use of the thermodynamic potentials, originally formulated in 1886 by Pierre Duhem. A different thermodyanmic potential exists for each combination formed by making each of the above variables either dyanamic or constant. Once one thermodynamic potential is known the others may be found by taking *Legendre transformations* of it, typically done with the *internal energy* U due to U having a well understood physical interpretation.

The particular thermodynamic potential which is of interest to us in the rest of the discussions to follow is the *Grand potential* Ω, and so all reference to the term *thermodynamic potential* will be used interchangeably with *Grand potential* beyond this section. The Grand potential has the following definition

$$\Omega = U - TS - \sum_i \mu_i N_i. \tag{2.1}$$

The quantity U can be found from considerations of the system available energy microstates, and this is done via a factor known as the *partition function*, which is simply the

sum of Boltzmann factors over all energy states [8]

$$Z(T) = \sum_s \exp(-\epsilon_s / k_B T) \tag{2.2}$$

where k_B is *Boltzmann's constant* and ϵ_s is the energy of state s. In Quantum Field Theory (QFT) it is given instead by the path integral on field configurations

$$\mathcal{Z} = \int D[\phi] \exp\left(i \int \frac{d^4k}{(2\pi)^4} \phi(-k) G^{-1}(k) \phi(k) \right) \tag{2.3}$$

where $G^{-1}(k)$ is the inverse field propagator.

One can verify that

$$\Omega = -T ln Z \tag{2.4}$$

is a solution to Eq (2.1) by also noting that

$$S = -\left(\frac{\partial \Omega}{\partial T}\right)_{V,\mu_i} \qquad N_i = -\left(\frac{\partial \Omega}{\partial \mu_i}\right)_{T,V,\mu_{j\neq i}}, \tag{2.5}$$

where the notation being used in the derivative subscripts is a list of variables being held constant for the partial derivative.

It will now be useful to define here the total derivative of the grand potential, which comes directly from Eq (2.1) and the total derivative of U

$$dU = TdS - pdV - \sum_i \mu_i dN_i, \tag{2.6}$$

which may be arranged into

$$d(U - TS - \sum_i \mu_i N_i) = -SdT - pdV - \sum_i N_i d\mu_i = d\Omega. \tag{2.7}$$

From Eq (2.7) we can now define the system pressure, which will be useful in later sections. One sees that in finding the partial derivative of the thermodynamic potential with

respect to volume

$$\frac{d\Omega}{dV} = -S\frac{dT}{dV} - p - \sum_i N_i \frac{d\mu_i}{dV}, \tag{2.8}$$

and by holding temperature and chemical potential constant, this leads to our definition for the pressure being

$$p = -\left(\frac{\partial\Omega}{\partial V}\right)_{T,\mu_i}, \tag{2.9}$$

and the definition for particle number

$$N_i = -\left(\frac{\partial\Omega}{\partial\mu_i}\right)_{T,V,\mu_{j\neq i}}, \tag{2.10}$$

which is akin to the particle density that will be used in later sections. Following a similar procedure used in deriving Eq (2.7) one can define

$$F = \Omega + \sum_i \mu_i N_i \tag{2.11}$$

which gives the free energy of the system.

2.2 Superconductivity

The first scientific observation of superconducting phenomena was made by Heike Kamerlingh Onnes in 1911 [2]. He observed that at extremely low temperatures, below a certain threshhold temperature, which depends on the conductors material, a current is able to flow without any resistance. However, this could be imagined as simply a perfect conductor, which was Onnes' motivation for studying the phenomenon. He was attempting to determine if the resistivity would vanish according to the Drude model, or whether it would actually increase as proposed by Lord Kelvin. Unexpectedly, however the resistance did not gradually drop but did so suddenly, hinting that this may be a new phenomenon at work. Onnes won the Nobel prize in 1913 for this research that led to the creation of liquid helium. However,

it wasn't until the discovery (of the so called Meissner effect) by Meissner and Ochsenfeld in 1933 [22], a complete expulsion of a magnetic field from the superconductor as its temperature drops below the critical value T_C, that physicsts realized a completely new theory of superconductivity would be required.

In any idealized perfect conductor an external magnetic field would be repelled by the simple creation of currents on its surface, which do not diminish in time due to zero resistance. These currents would generate an induced magnetic field that would completely oppose any external magnetic field. However, this is not, in general, the behaviour observed in superconductors. As stated above, the expulsion of the magnetic field inside the conductor, up to a distance from the surface known as the *London penetration depth*, by an opposing one is set up at the moment the superconductor drops below the threshhold temperature and bemes a superconductor. This induced magnetic field is permanent and does not account for any new changes in external magnetic fields, and therefore the currents set up at the creation of the superconductor are known as *persistent currents*.

A microscopic theory of superconductivity, known as *BCS theory* after its creators Bardeen, Cooper, and Schrieffer, was published in 1957 for which they shared a Nobel prize. A normal superconductor allows electrical current to flow through it with no resistance. This occurs because vibrations of the lattice, mediated by *phonons*, can give rise to a net attractive force between electrons that are relatively far apart. The resulting bound state is called a Cooper pair composed of two electrons of half spin, giving the Cooper pair a spin of zero and can hence be described as a boson. Being bosons, the Cooper pairs may condense to the same energy state leaving behind an energy gap for the quasiparticles. Once this gap is created, electron energies can be freely exited up into the gap allowing them to move freely without resistance. In doing so, the electrons simultaneously leave behind a hole, which may be thought of as a positively charged particle. Note that all of this depends on the delicate phonon interaction that can be disturbed by thermal effects. This is the reason why all known superconductors require low temperatures.

2.3 QCD

Quantum Chromodynamics (QCD) is a theory describing the behaviour of particles that possess *color charge*. Unlike other fundamental forces, the interaction mediating particles in QCD are not neutral. *Gluons* are the force mediators and their charge is described with a color and an anti-color. Particles in color bound states have oscillating color charge due to constant gluon interactions and the fact that they only posses a single color charge. The effect of the gluons color/anti-color charge is to change the charge of the particle it interacts with.

In a system of fermions at zero temperature, $T = 0$, all the fermions are in their lowest energy states. However, unlike bosons, which are *integral spin* particles, fermions are *half-integer spin* particles, and so in accordance with the *Pauli exclusion principle*, particles with half-integer spin cannot occupy the same quantum state as each other. Therefore, the ground state of a system of fermions is the state in which all of the N lowest individual fermion states are occupied, where N is the total number of identical fermions in the system. The distribution for fermions is known as the *Fermi-Dirac* distribution function [15]

$$f(\epsilon_{k_0}) = \frac{1}{e^{\beta(\epsilon_{k_0}-\mu)} + 1} \tag{2.12}$$

with $\beta = 1/(k_B T)$. Taking the limit of Eq (2.12) as T approaches zero yields either $f(\epsilon_{k_0}) = 1$ or 0, depending on whether $\mu - \epsilon_{k_0} > 0$ or $\mu - \epsilon_{k_0} < 0$, respectively. These two regions can be summarized as a single expression by using an *Heaviside step function*

$$f(\epsilon_{k_0}) = \theta(\mu - \epsilon_{k_0}), \tag{2.13}$$

so that all states up to a critical value of $\epsilon_{k_0} = \mu$ are filled. This critical value is known as the *Fermi energy*. The corresponding momentum k which produces this energy, coming from the relation

$$\epsilon_{k_0} = \sqrt{k^2 + m^2} = \mu, \tag{2.14}$$

is known as the *Fermi momentum* k_F, or P_F as it will be labeled later. Because the momentum enters into the energy function as a square, k^2, and if we take the Fermi momentum to be very large, then in momentum space the boundary between occupied and empty states may be approximated as a sphere, the *Fermi sphere* with a radius of P_F giving a total volume of $\frac{4}{3}\pi P_F^3$ in momentum space. The Fermi energy then is taken to have infinite degeneracy, due to having approximately infinite points on the surface at the same energy level.

As outlined previously (Section 2.2) there exists between fermions near the surface an attractive interation. Then, as Cooper showed [7], regardless of how weak this interation is the tendency of the fermions will be to form bound Cooper pairs. Being composed of two individual half-integer spin particles the Cooper pair can be thought of as a *composite boson* because the resulting combination will have whole integer spin. The Cooper pairs then together form a particle which is not subject to the Pauli exclusion principle, and so all of them may condense to the same ground state.

2.4 QCD Phase Diagram

Figure 2.1 is a schematic representation in the temperature-density plane of known phases of QCD [10].

At baryonic chemical potential around $\mu_{NM} = 924MeV$ and $T = 0$ nuclear matter starts to form, and in this region of the graph the familiar critical point of a phase transition between the familiar hadronic matter, mesons and baryons, makes up the low temperature and low density corner of the graph. In the outer regions of the temperature density plane, our current understanding only allows us to make strong statements on limiting cases, such as high T and relatively small density or, as in this thesis, asympotically high density and low vanishing T. The first of these cases leads to a region of deconfinement where individual quarks are too energetic to remain in bound states from the strong nuclear interaction which is the state of matter thought to have existed in the early universe and known as the *quark-gluon plasma* (QGP).

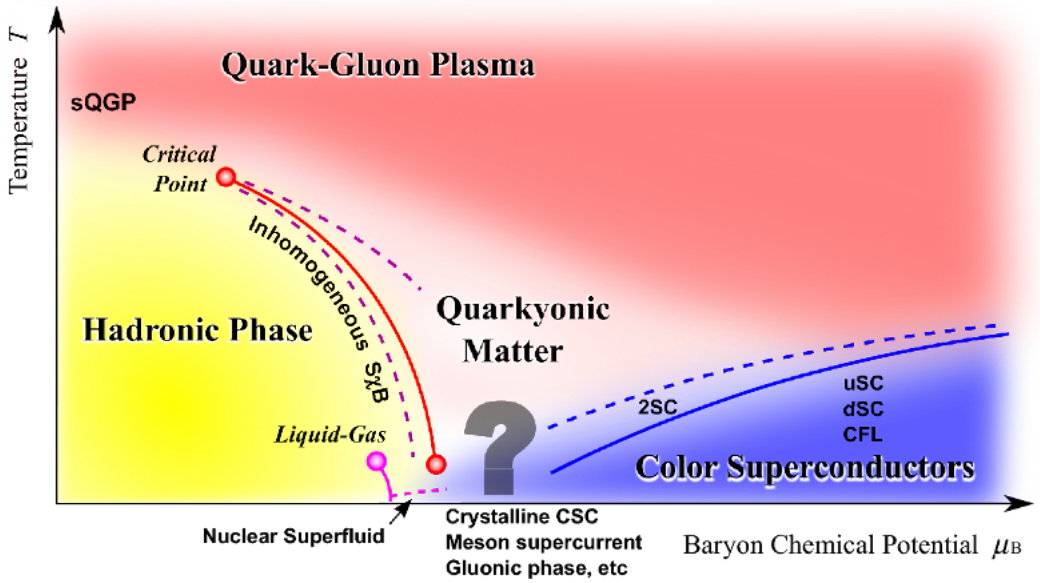

Figure 2.1: QCD Phase Diagram

There is a phase transition for finite temperature and zero chemical potential which has been extensively studied numerically. There is a crossover for a pseudo-critical temperature T_{pc} according to recent analyses [23][24] within the range $150MeV - 200MeV$ [10]. This high T region corresponds to the QGP. The second limiting case is a color superconducting state of cold quark matter existing as a system of Cooper pairs forming the CFL phase. Not much is known however about the transition from the color superconducting region to condensed hadronic matter. As has been discussed earlier in this thesis, a smooth crossover to the formation of Bose molecules can occur when the diquark interaction becomes stronger at moderate densities.

There is a critical point denoted in Fig. 2.1 for high T, above which shows a region governed by a smooth transition toward the QGP. Crossing the intermediate line between hadronic matter and the QGP yields a phase transition. However, the bottom regions of the plane, at relatively low T and intermediate densities might imply another smooth crossover rather than a phase transitions. Not much information can be derived from first principle in either of these intermediate crossover regions.

We will want to investigate how equations of state behave throughout the BCS-BEC crossover in order to understand how the dynamical properties of our systems will change.

2.5 BCS-BEC crossover

The attraction binding ultracold fermionic pairs in atomic physics can be tuned via Feshbach resonance where an applied magnetic field is used to adjust the interaction. Crossovers between BCS and BEC dynamics have already been observed [2]. In tuning the interaction the coherence length of the Cooper pairs is altered. In the BCS regime the coherence length is much larger than the interparticle spacing. However, for BEC dynamics to occur at larger coupling strength that can reducing the interparticle distance enough to form Bose molecules, the fermionic degrees of freedom have to be removed.

As for dense quark matter in particular, strong theoretical developments now exist indicating that by tuning the interaction strength between the quarks forming the Cooper pairs we can drive the system between domains of BCS and BEC dynamics [5], and several models have already been proposed [17]-[21]. This section serves to introduce a general layout for the methods and definitions used in defining the crossover parameter in the models presented later in Chapters 3 and 4

The Pauli exclusion principle prevents half-integer spin particles from occupying the same quantum states, however, bosons having integral spin means they are not subject to this restriction. Therefore, a uniformly distributed system of bosons may act as free particles giving rise to color superconductivity. Color superconductivity can also be realized for a system of fermions according to BCS theory by the formation of Cooper pairs composed of different color quarks [9] with opposite momentum near the Fermi-surface. Now, let us discuss in a simple way how the BCS-BEC crossover takes place in a relativistic system [3].

The dispersion of the quasiparticles in a superconductor is given by

$$\epsilon_k = \sqrt{(\epsilon_{k_0} - \mu)^2 + \Delta^2} \tag{2.15}$$

where for relativistic energies

$$\epsilon_{k_0} = \sqrt{m^2 + k^2}. \tag{2.16}$$

From Eq. (2.15) we find that the energy minimum in k has two values, one at $k = \sqrt{\mu^2 - m^2}$ and another at $k = 0$. It can be seen that the minimum at $k = \sqrt{\mu^2 - m^2}$ results in a lower energy than that at $k = 0$, and is thus the true minimum provided that $\mu \geq m$. However, if $\mu \leq m$ then the first minima disappears due to not returning a real value, leaving $k = 0$ as the minimum. With the first minima we have an energy gap Δ as is the case for a BCS state, while the second minima leaves an energy gap of $\sqrt{(m-\mu)^2 + \Delta^2}$ which corresponds to a BEC state of matter. Because the two minima, as well as the energy gaps for both BCS and BEC, are equal for $\mu = m$ this suggests a smooth crossover between the two regions rather than an abrupt phase transition.

2.6 Newton's Method

In chapters 3 and 4 it will become necessary to solve systems of integral equations for the energy gap (Δ) and chemical potential (μ) which require us to resort to numerical techniques. One such technique is called *Newton's method*, which we will use in this section to derive a solution that may be applied to the specific cases that will arise later.

Newton's method is a technique for finding approximately the roots for equations of the form $f(x) = 0$. For functions of a single variable Newton's method is summarized in the following iterative equation

$$x_{n+1} = x_n - \frac{f(x_n)}{f'(x_n)} \tag{2.17}$$

where x_{n+1} is a better approximation to the true solution than was x_n. x_0 is often chosen as a best guess, or in order to ensure convergence of the series. For systems of equations involving more than one variable of the form $f_i(\mathbf{x}) = 0$ where $\mathbf{x}$ is a column vector, and each

of the $f_i(\mathbf{x})$ is an element in the column vector $\mathbf{F}$, then Eq (2.17) becomes

$$\mathcal{J}\mathbf{y} = \mathbf{F} \tag{2.18}$$

in which $\mathcal{J}$ is the Jacobian matrix having elements

$$\mathcal{J}_{ij} = \frac{\partial F_i}{\partial x_j} \tag{2.19}$$

and $\mathbf{y}$ is the column vector $\mathbf{y} = \mathbf{x}_{n+1} - \mathbf{x}_n$ representing the correction to $\mathbf{x}_n$ for each iteration.

In the special case in which we have a system of two equations with two variables, meaning $\mathbf{F}$ and $\mathbf{y}$ are 2 component vectors and the Jacobian, $\mathcal{J}$, is a 2×2 matrix, then a general solution can be found for y_1 and y_2, as

$$\begin{aligned} y_1 &= \left(\tfrac{\mathcal{J}_{22}}{\mathcal{J}_{12}} F_1 - F_2\right) \tfrac{\mathcal{J}_{12}}{\mathcal{J}_{12}\mathcal{J}_{21} - \mathcal{J}_{11}\mathcal{J}_{22}} \\ y_2 &= -\tfrac{F_1 + \mathcal{J}_{11} y_1}{\mathcal{J}_{12}}. \end{aligned} \tag{2.20}$$

The above equations is our general solution which will be used in Chapters 3 and 4 to solve the systems of integral equations. The integrals themselves will also be solved numerically using the *trapezoidal rule*. The final values, $\mathbf{y}$, are then added to $\mathbf{x}_n$ and the process is repeated until

$$\mathbf{F} \leq \epsilon, \tag{2.21}$$

where ϵ is an acceptably low error.

Chapter 3

Equations of State in a Relativistic Boson-Fermion System

This Chapter studies the BCS-BEC crossover for color superconducting regimes by using a relativistic model that possesses both bosonic and fermionic degrees of freedom [20]. Therefore, it is expected that the density of fermions should vanish when entering the BEC region and vice versa. This is in contrast to the purely fermionic model presented in Chapter 4 in which there is only fermionic degrees of freedom.

3.1 Composite-Boson-Fermion model

The bosons are expected to form at lower densities when asymptotic freedom is broken and the quarks are no longer able to exist as free particles. In that case, quarks bind together into diquark molecules. In this model we treat independently the boson molecules that exist in the strong coupling regime, and the composite diquarks which are expected to form as Cooper pairs in the weak coupling regime. They will appear as different fields contributing to the Lagrangian. We will refer to the system as either being BCS or BEC based on which dispersion relation (Eq (3.8) and graphed in Fig. 3.2) describes the quasiparticles in each region in question. The Lagrangian is composed of a bosonic ($\mathcal{L}_0$) and fermionic ($\mathcal{L}_F$) term with a Yukawa interaction between the two ($\mathcal{L}_I$):

$$\mathcal{L} = \mathcal{L}_f + \mathcal{L}_b + \mathcal{L}_I \tag{3.1}$$

where

$$\begin{aligned}\mathcal{L}_f &= \bar{\psi}\left(i\gamma^\mu\partial_\mu + \gamma_0\mu - m\right)\psi \\ \mathcal{L}_b &= |\left(\partial_t - i\mu_b\right)\varphi|^2 - |\nabla\varphi|^2 - m_b|\varphi|^2 \\ \mathcal{L}_I &= g\left(\varphi\bar{\psi}_C i\gamma_5\psi + \varphi^*\bar{\psi}i\gamma_5\psi_C\right)\end{aligned} \tag{3.2}$$

Here, $C = i\gamma^2\gamma^0$ is the charge conjugate matrix, and $\psi_C = C\bar{\psi}^T$ and $\bar{\psi}_C = \psi^T C$ are the charge conjugate spinors. We also impose the restriction that $\mu_b = 2\mu$ to ensure equilibrium between fermion and boson conversions. Then, in the mean-field approximation in which $\phi = \langle\varphi_0\rangle$ is the vaccuum expectation value of the boson field, we find in the Nambu-Gorkov space with spinors

$$\Psi = \begin{pmatrix} \psi \\ \psi_C \end{pmatrix}, \qquad \bar{\Psi} = \left(\bar{\psi}, \bar{\psi}_C\right) \tag{3.3}$$

the Lagrangian density

$$\mathcal{L} = \frac{1}{2}\bar{\Psi}\mathcal{S}^{-1}\Psi + (\mu_b^2 - m_b^2)|\phi|^2 + |(\partial_t - i\mu_b)\phi|^2 - |\Delta\phi|^2 - m_b^2|\phi|^2 \tag{3.4}$$

with inverse fermion propagator given by

$$\mathcal{S}^{-1}(P) = \begin{pmatrix} P_\mu\gamma^\mu + \mu\gamma_0 - m & 2ig\gamma_5\phi^* \\ 2ig\gamma_5\phi & P_\mu\gamma^\mu - \mu\gamma_0 - m \end{pmatrix}. \tag{3.5}$$

As it is characteristic of the mean-field approximation we neglect the interaction between the fermions and the fluctuating boson fields.

The thermodyanmic potential density at finite temperature T is then computed beginning with the partition function from Eq. (2.3). In our case with fermionic and bosonic fields this is

$$Z = \int [d\psi][d\bar{\psi}][d\phi][d\phi^*] e^{\int_0^{1/T} d\tau d^3x \mathcal{L}}. \tag{3.6}$$

Plugging the above into Eq. (2.4) yields

$$\begin{array}{c}\Omega = -\sum_{e=\pm}\int \frac{d^3k}{(2\pi)^3}\left[\epsilon_k^e + 2Tln\left[1+exp\left(-\frac{\epsilon_k^e}{T}\right)\right]\right] + \frac{(m_b^2-\mu_b^2)\Delta^2}{4g^2} \\ +\frac{1}{2}\sum_{e=\pm}\int \frac{d^3k}{(2\pi)^3}\left[\omega_k^e + 2Tln\left[1-exp\left(\frac{-\omega_k^e}{T}\right)\right]\right],\end{array} \quad . \tag{3.7}$$

where the terms involving the quasiparticle energy are denoted by

$$\epsilon_k^e = \sqrt{\left(\epsilon_{k0} - e\mu\right)^2 + \Delta^2} \qquad \epsilon_{k0} = \sqrt{k^2+m^2} \qquad \omega_k^e = \sqrt{k^2+m_b^2} - e\mu_b, \tag{3.8}$$

with $e = \pm 1$ corresponding to fermions and antifermions for plus and minus respectively, and $\Delta = 2g\phi$. We are particularly interested in the zero-temperature limit of the thermodynamic potential

$$\Omega_0 = -\sum_{e=\pm}\int \frac{d^3k}{(2\pi)^3}\epsilon_k^e + \frac{\left(m_b^2-\mu_b^2\right)\Delta^2}{4g^2} + \frac{1}{2}\sum_{e=\pm}\int \frac{d^3k}{(2\pi)^3}\omega_k^e. \tag{3.9}$$

In this model we renormalize the boson mass rather than the coupling, by the condition

$$m_{b,r}^2 = 4g^2\left.\frac{\partial\Omega}{\partial\Delta^2}\right|_{\Delta=\mu=T=0} = m_b^2 - 4g^2\int\frac{d^3k}{(2\pi)^3}\frac{1}{\epsilon_{k_0}}. \tag{3.10}$$

The crossover parameter that will be used is defined as follows

$$x = -\frac{m_{b,r}^2-\mu_b^2}{4g^2}, \tag{3.11}$$

Hence, from Eqs. (3.10) and (3.11) the dynamical boson mass is given in terms of the crossover parameter as

$$m_b^2 - \mu_b^2 = 4g^2\left(\int\frac{d^3k}{(2\pi)^3}\frac{1}{\epsilon_{k_0}} - x\right) = 4g^2(x_0 - x). \tag{3.12}$$

Then, for small enough fermion masses ($m \ll \Lambda$, where Λ is the momentum cutoff), we have

$$x_0 \approx \frac{\Lambda^2}{4\pi^2}. \tag{3.13}$$

3.2 Gap Equation at Fixed Fermion Density

Now, to find solutions for μ and Δ we can make use of two additional conditions. First, because each momentum state in the Fermi sphere can only be occupied by two fermions of opposite spin, there exists a relation between the particle density in momentum space and the Fermi momentum. The second condition is that the energy gap produced by the Cooper pairs should minimize the thermodynamic potential. These two conditions are summarized in the following equations respectively

$$\frac{\partial \Omega_0}{\partial \mu} = -\frac{P_F^3}{3\pi^2} \tag{3.14}$$

$$\frac{\partial \Omega_0}{\partial \Delta} = 0. \tag{3.15}$$

Substituting Eq. (3.9) into the above yields

$$\left(\frac{P_F^3}{3\pi^2}\right) = \frac{1}{2\pi^2}\int_0^1 k^2 dk \left[\frac{\xi_k^+}{\epsilon_k^+} - \frac{\xi_k^-}{\epsilon_k^-}\right] + \frac{2}{g^2}\mu\Delta^2 \tag{3.16}$$

$$-\frac{x}{x_0} = 2\int_0^1 k^2 dk \left[\frac{1}{\epsilon_k^+} + \frac{1}{\epsilon_k^-} - \frac{2}{\epsilon_{k_0}}\right] \tag{3.17}$$

with

$$\xi_k^e = \epsilon_k - e\mu. \tag{3.18}$$

3.3 Numerical Solutions

To solve the set of Eqs. (3.16)-(3.17) we resort to numerical methods with the following parameters fixed: the upper limit of momentum $\Lambda = 602.3\text{MeV}$, $P_F = 0.3\Lambda$, $m = 0.4\Lambda$, and $g = 4/\Lambda^2$. The procedure now follows the methods described in section 2.6 to adapt them

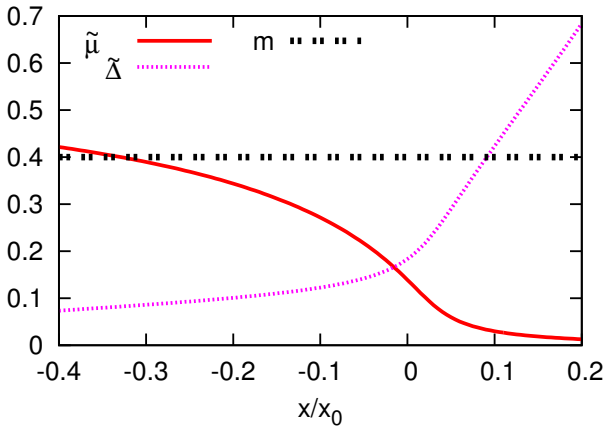

Figure 3.1: $\tilde{\mu}$ and $\tilde{\Delta}$ vs. the crossover parameter x/x_0, where $\tilde{\mu} = \mu/\Lambda$ and $\tilde{\Delta} = \Delta/\Lambda$

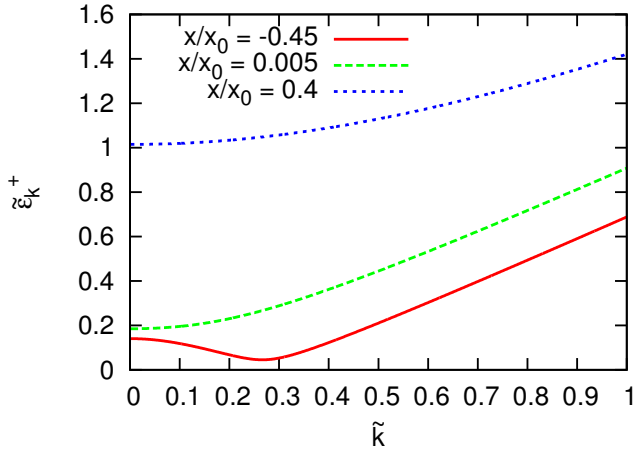

Figure 3.2: Quasiparticle dispersion curves of Eq. (3.8) for various values of x/x_0

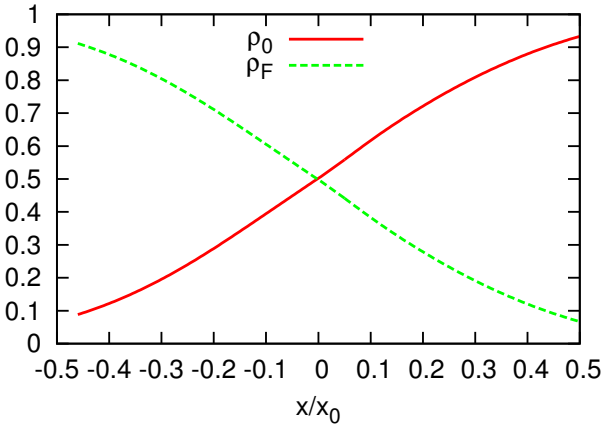

Figure 3.3: Boson and fermion densities, ρ_0 and ρ_F respectively, vs. the crossover parameter x/x_0

for this model. Here the column vector $\mathbf{F}$ of equation (2.18) has elements

$$\begin{aligned} F_1 &= \tfrac{3}{2}\int_0^1 k^2 dk \left[\frac{\xi_k^-}{\epsilon_k^-} - \frac{\epsilon_k^+}{\epsilon_k^+}\right] + \frac{6\pi^2}{g^2}\mu\Delta^2 - P_F^3 \\ F_2 &= \int_0^1 k^2 dk \left[\frac{1}{\epsilon_k^+} + \frac{1}{\epsilon_k^-} - \frac{2}{\epsilon_{k_0}}\right] + \frac{x}{x_0} \end{aligned} \tag{3.19}$$

The elements of $\mathbf{x}$ are then μ and Δ, the error value for Eq. (2.21) was set to 10^{-7}, and the Jacobian matrix $\mathcal{J}$ were found to be

$$\begin{aligned} \mathcal{J}_{11} &= \tfrac{3}{2}\int_0^1 k^2 dk \left[\frac{1}{\epsilon_k^+} + \frac{1}{\epsilon_k^-} - \frac{(\xi_k^+)^2}{(\epsilon_k^+)^3} - \frac{(\xi_k^-)^2}{(\epsilon_k^-)^3}\right] + \frac{6\pi^2}{g^2}\Delta^2 \\ \mathcal{J}_{12} &= \tfrac{3}{2}\int_0^1 k^2 dk \left[\frac{\xi_k^+}{(\epsilon_k^+)^3} - \frac{\xi_k^-}{(\epsilon_k^-)^3}\right] + \frac{12\pi^2}{g^2}\mu\Delta \\ \mathcal{J}_{21} &= \int_0^1 k^2 dk \left[\frac{\xi_k^+}{(\epsilon_k^+)^3} - \frac{\xi_l^-}{(\epsilon_k^-)^3}\right] \\ \mathcal{J}_{22} &= -\int_0^1 k^2 dk \left[\frac{1}{(\epsilon_k^+)^3} + \frac{1}{(\epsilon_k^-)^3}\right]\Delta, \end{aligned} \tag{3.20}$$

We can then readily apply the general solution, Eq. (2.20), together with the numerical integration described in that section to find our solutions.

The obtained solutions of μ and Δ have been graphed in Fig. 3.1. With these solutions we can readily determine the EoS for this model. We start by plotting the quasiparticle's dispersion relation from Eq. (3.8), as seen in Fig. 3.2. One interesting consequence of this

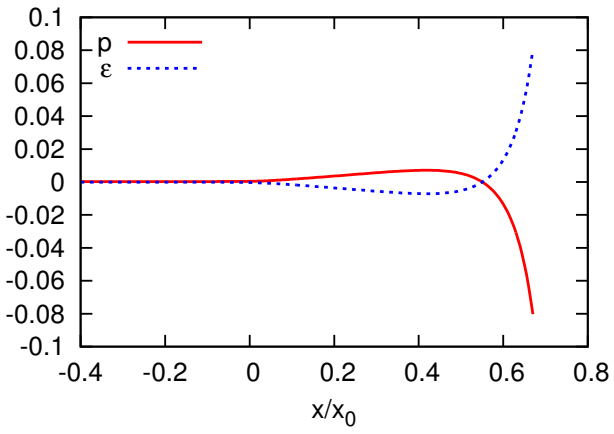

Figure 3.4: Pressure and energy density $\tilde{p} = p/\Lambda^4$ $\tilde{\epsilon} = \epsilon/\Lambda^4$ vs. the crossover parameter x/x_0.

graph is that according to the explanation in section 2.4, we observe a bosonic like curve for x/x_0 larger than the critical value where the system crosses over to the BEC regime, as indicated by the chemical potential becoming smaller than th mass in Fig. 3.1. This means that even though we model the system as separate boson and fermion contributions the quasiparticles behave as bosons in the strong coupling regime.

Now we investigate the system EoS using the solutions for chemical potential and gap just found. The energy density and pressure are given respectively by $\epsilon = \Omega_0 + \mu n$ and $p = -\Omega_0$. To guarantee that the system pressure and energy become zero in vacuum (i.e. when $\mu = \Delta = 0$) we introduce

$$\begin{aligned} \epsilon &= \Omega_0 + \mu n - \Omega_0^{\text{vac}} \\ p &= -\Omega_0 + \Omega_0^{\text{vac}} \\ \Omega_0^{\text{vac}} &= \Omega_0(\mu = \Delta = 0). \end{aligned} \tag{3.21}$$

Next we analyze with the fractional densities of fermions ($\rho_F = n_F/n$) and bosons ($\rho_0 = n_0/n$), such that $n = n_0 + n_F$, where

$$n_F = -\frac{\partial \Omega}{\partial \mu}, \qquad n_0 = \frac{2\mu\Delta^2}{g^2}, \qquad n = \frac{P_F^3}{3\pi^2}. \tag{3.22}$$

As you can see in Fig. 3.3 the system is primarily composed of fermions with a low boson density when $x/x_0 < 0$, highlighting the BCS portion of the x/x_0 domain, while in the right half of the graph, for $x/x_0 > 0$, there consists of a high boson and low fermion density corresponding to the BEC region.

The numerical solutions previously found are now used to examine the EoS (i.e. the pressure and energy), displayed in Fig. 3.4. The dominant term in Ω_0 is the bosonic contribution throughout both BCS and BEC regimes, however, once the vacuum term Ω_{vac} is subtracted the bosonic contribution essentially disappears. The sign in the middle term of Eq. (3.9) is determined by $m_b^2 - \mu_b^2$ which changes roughly around the crossover when $\mu = m$. So the middle term contributes a positive pressure to the BCS region, yet turns negative just before the crossover to the BEC region. As for the fermionic contribution to the pressure, it is positive throughout both regions. Therefore, it is this middle, fermion-boson interaction, term which makes the pressure unstable in the far BEC region.

Further investigation shows that the same results as above may also be obtained for various values of m and m_b. The values used in this thesis were chosen to agree with the originally proposed model [20], as well as to highlight the pressure instability that may occur in the far BEC regime. These two considerations required careful balancing due to limitations of the numerical methods used. Additionally, the presence of a positive pressure in the BCS region with a decreasing pressure, together with the instability, toward the BEC region agree with expectations, because of the lack of Pauli exclusion principle once the quasiparticles become bosonic.

Chapter 4

Fermionic Model for a Relativistic Superfluid

This model describes a system with only fermionic degrees of freedom and multi-fermion interactions. The attractive channel between quarks allows the formation of diquarks in the strong coupling regime. The diquarks play the role of the bosonic field used in chapter 3. Additionally there exists a diquark-diquark repulsive channel [16] parameterized by the coupling constant λ.

4.1 Purely-Fermionic model

For this investigation we consider a simple relativistic model of fermions with multi-fermion interactions represented in the Lagrangian density

$$\mathcal{L} = \bar{\psi}\left(i\gamma^{\mu}\partial_{\mu} - m\right)\psi + \mathcal{L}_I + \mathcal{L}'_I \tag{4.1}$$

where

$$\mathcal{L}_I = \frac{g}{4}\left(\bar{\psi}i\gamma_5 C\bar{\psi}^T\right)\left(\psi^T C i\gamma_5\psi\right)$$

$$\mathcal{L}'_I = -\lambda\left[\left(\bar{\psi}i\gamma_5 C\bar{\psi}^T\right)\left(\psi^T C i\gamma_5\psi\right)\right]^2,$$

m is the fermion mass, μ the chemical potential, g the fermion-fermion coupling constant, λ the diquark-diquark repulsive constant, and $C = i\gamma_0\gamma_2$ the charge conjugation matrix.

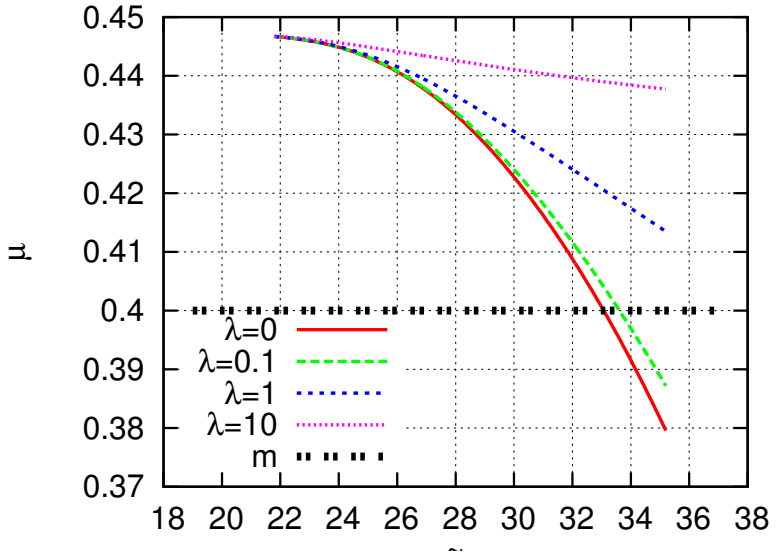

Figure 4.1: Chemical potential μ versus coupling constant $\tilde{g} = g\Lambda^2$ plotted for different values of λ.

With $\mathcal{L}_I$ above simulating the quark-quark attractive interaction and the second, primed, term $\mathcal{L}'_I$ with $\lambda > 0$ corresponding to a diquark-diquark repulsive interaction. From this Lagrangian density (4.1) and the procedure outlined in Section 2.4 the thermodynamic potential can be calculated [20], which at $T = 0$ is

$$\Omega_0 = -\sum_{e=\pm 1} \int_\Lambda \frac{d^3k}{(2\pi)^3} \epsilon_k^e + \frac{\Delta^2}{g} + \lambda\Delta^4 \tag{4.2}$$

With the energy spectrum, ϵ_k^e, given by

$$\epsilon_k^e = \sqrt{(\epsilon_{k_0} - e\mu)^2 + \Delta^2} \tag{4.3}$$

$$\epsilon_{k_0} = \sqrt{k^2 + m^2}$$

and $e = \pm 1$, which corresponds to particles for positive, and antiparticles for negative.

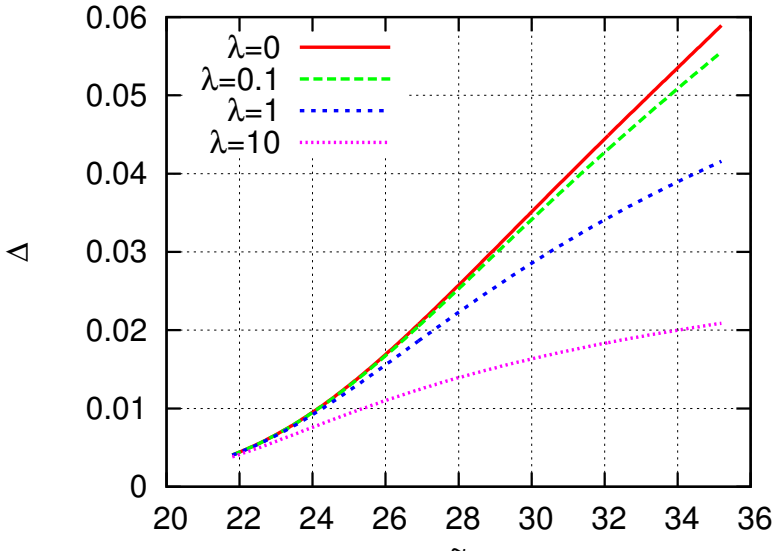

Figure 4.2: Energy gap Δ versus coupling constant $\tilde{g} = g\Lambda^2$ plotted for different values of λ.

4.2 Numerical solutions

Similar to Chapter 3, the goal is now to find solutions for μ and Δ from the thermodynamic potential, Eq. (4.2). This is done with the particle density equation fixed by the Fermi momentum

$$P_F^3 = 3\pi^2 \frac{\partial \Omega_0}{\partial \mu} = -\frac{3}{2} \int_\Lambda dk k^2 \left[\frac{\xi_k^+}{\epsilon_k^+} - \frac{\xi_k^-}{\epsilon_k^-} \right] \tag{4.4}$$

and the gap equation $\partial\Omega_0/\partial\Delta = 0$ that can be written as

$$1 = \frac{g}{4\pi^2} \int_\Lambda dk k^2 \left[\frac{1}{\epsilon_k^+} + \frac{1}{\epsilon_k^-} \right] - 2\lambda g \Delta^2 \tag{4.5}$$

where

$$\xi_k^e = \epsilon_k - e\mu \tag{4.6}$$

Once more employing the general solution of Eq. (2.20) we have

$$\begin{aligned} F_1 &= \tfrac{3}{2} \textstyle\int_0^1 dk k^2 \left[\frac{\xi_k^-}{\epsilon_k^-} - \frac{\xi_k^+}{\epsilon_k^-} \right] - \left(\frac{P_F}{\Lambda} \right)^3 \\ F_2 &= \tfrac{g}{4\pi^2} \textstyle\int_0^1 dk k^2 \left[\frac{1}{\epsilon_k^+} + \frac{1}{\epsilon_k^-} \right] - 2\lambda g \Delta^2 - 1 \end{aligned} \tag{4.7}$$

and the elements of the Jacobian

$$\begin{aligned}
\mathcal{J}_{11} &= \tfrac{3}{2}\int_0^1 dk k^2 \left[\tfrac{1}{\epsilon_k^+} + \tfrac{1}{\epsilon_k^-} - \tfrac{(\xi_k^+)^2}{(\epsilon_k^+)^3} - \tfrac{(\xi_k^-)^2}{(\epsilon_k^-)^3}\right] \\
\mathcal{J}_{12} &= \tfrac{3}{2}\int_0^1 dk k^2 \left[\tfrac{\xi_k^+}{(\epsilon_k^+)^3} - \tfrac{\xi_k^-}{(\epsilon_k^-)^3}\right]\Delta \\
\mathcal{J}_{21} &= \tfrac{g}{4\pi^2}\int_0^1 dk k^2 \left[\tfrac{\xi_k^+}{(\epsilon_k^+)^3} - \tfrac{\xi_k^-}{(\epsilon_k^-)^3}\right] \\
\mathcal{J}_{22} &= -\tfrac{g}{4\pi^2}\int_0^1 dk k^2 \left[\tfrac{1}{(\epsilon_k^+)^3} + \tfrac{1}{(\epsilon_k^-)^3}\right]\Delta - 4\lambda g\Delta
\end{aligned} \tag{4.8}$$

In solving this system of integral equations we fix the other parameters to represent a relativistic quark gas [19], $\Lambda = 602.3$MeV the cutoff in the momentum integral, $m/\Lambda = 0.4$ the fermionic mass, and $P_F/\Lambda = 0.3$ the Fermi momentum, and the results are graphed in Figs. 4.1 and 4.2. To verify the BCS-BEC crossover from the dynamics of the quasiparticles we have plotted the energy spectrum of Eq. (4.3) in Fig. 4.3 for a few values of the coupling strength. Then in accordance with Section 2.5 looking at Eq. (4.3), with $\mu > m$ the value of the momentum k which minimizes the energy spectrum is $k = \sqrt{\mu^2 - m^2}$ (non-zero) and the energy gap is simply Δ, but for $\mu < m$ the momentum must be zero to minimize the energy leaving a gap of $\sqrt{(m-\mu)^2 + \Delta^2}$. Figure 4.3 is consistent with this, noting from Fig. 4.1 that μ varies inversely with g, we see that the minimum in the energy spectrum for a stronger value of g is at $k = 0$ which indicates a bosonic state, whereas k is non-zero for lower values of g, indicating a BCS region. Therefore treating g as the crossover parameter to move the system between the two regions is justified, and a critical value for the crossover can be defined, $g_{\text{cr}} = 33/\Lambda^2$.

4.3 Stability Condition in the BEC Region

Finally, we are ready to use the above solutions for μ and Δ to calculate the system pressure and energy

$$\epsilon = (\Omega_0 - B) + \mu n_0, \qquad p = -(\Omega_0 - B) \tag{4.9}$$

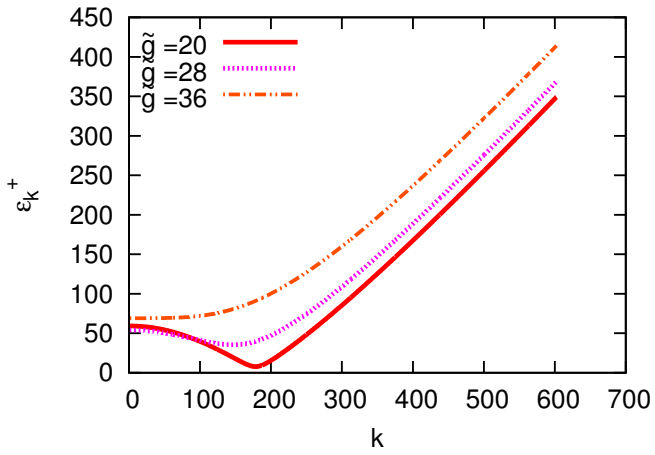

Figure 4.3: ϵ_k^+ vs k plotted for different values of the coupling strength $\tilde{g} = g\Lambda^2$.

where in this model the vacuum is treated as a constant, B, whose value is determined by setting the pressure to zero. Pressure is plotted in Fig. 4.4, and as can be seen the $\lambda = 0$ solution becomes negative before the critical value ($g_{\rm cr} = 33/\Lambda^2$), therefore this solution doesn't allow for BEC dynamics at all due to unstable pressure. Although a similar comparison shows that the other solutions for larger values of λ do permit BEC dynamics with positive pressure in this particular model.

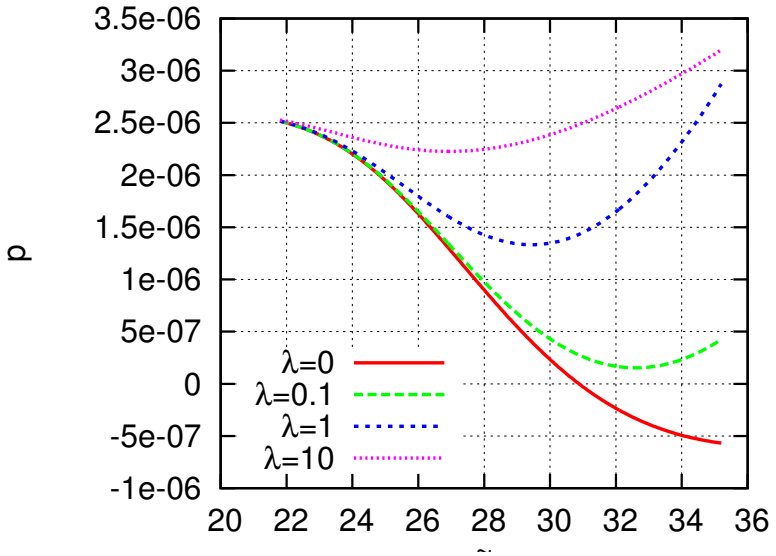

Figure 4.4: Pressure versus the coupling constant $\tilde{g} = g\Lambda^2$ for various values of λ.

Chapter 5

Final Remarks

We study the BCS-BEC crossover for two relativistic systems. One formed by fermions and bosons interacting through a Yukawa potential. The other, only having fermionic degrees of freedom under multi-fermion interactions that account for a fermion-fermion attractive channel and a difermion-difermion repulsion. The main goal of this investigations was to analyze the evolution of the system EoS throughout the crossover.

We have found for the boson-fermion model that the system pressure is positive throughout the entire BCS domain. In the BEC domain the pressure decreases to negative values indicating an instability. Before this instability occurs in the BEC region the pressure is positive and the graph actually displays an interesting downward concavity in the curve. In separating out the individual contributions to the pressure from each term it is observed that this inflection point is caused by a shift in dominance from the fermionic term given by an integral over the fermionic dispersion to the term contributed by the fermion-boson interaction (middle term) in Eq. (3.9).

In our simple fermion model the pressure displayed the expected decreasing behavior when the system crosses over from the BCS to the BEC region. In the case in which the diquark-diquark repulsion term was added to the thermodynamic potential it seems possible that the system could remain stable for all values of the coupling, g, in the BEC region [25]. Therefore, in this simple fermionic model we observe a stable BCS region which crosses over into stable BEC dynamics once the diquark-diquark repulsion is strong enough. However, our investigation was limited up to the $\lambda\Delta^4$ tree-level contribution. A more detailed investigation would introduce additional terms to the quasiparticle spectrum.

It appears the the two models are qualitatively in agreement as to the stability of the

star, with both stable BCS and BEC dynamics and an eventual instability arising deeper into the BEC region. One difference between the results that stands out is the existence of a maximum in the pressure in the middle of the BEC region for our fermion-boson model, wheras no such maximum exists in the simple fermion model. In the limit of low chemical potential, which is the case near this maximum, it can be seen that the equations describing the pressure in the two models becomes very similar. Yet, this difference between the two models still occurs due to the fact that the diquark-diquark repulsion in the simple fermion model enters into the calculations of μ and Δ as seen in Eq. (4.8).

As a physical interpretation of the instabilities described in this paper, note that the instabilities are thought to merely indicate where the model no longer describes a diquark BEC state, rather than an actual instability in the star. The graphs show that the instabilities would exist at lower densities within the neutron star which could possibly mean that the density is low enough for hadronization to take place.

References

[1] D. J. Gross and F. Wilczek, Phys. Rev. Lett. **30**, 1343 (1973).

[2] K. I. Wysokinski, arXiv:1111.5318 [physics.hist-ph].

[3] G. -f. Sun, L. He and P. Zhuang, Phys. Rev. D **75**, 096004 (2007) [hep-ph/0703159].

[4] E. J. Ferrer, V. de la Incera, J. P. Keith, I. Portillo and P. L. Springsteen, Phys. Rev. C **82**, 065802 (2010) [arXiv:1009.3521 [hep-ph]].

[5] M. Randeria and E. Taylor, Physics **5**, 209 (2014) [arXiv:1306.5785 [cond-mat.quant-gas]].

[6] I. A. Shovkovy, Found. Phys. **35**, 1309 (2005) [nucl-th/0410091].

[7] L. N. Cooper, Phys. Rev. **104**, 1189 (1956).

[8] C. Kittel and H. Kroemer, W. H. Freeman and Company, 1980, New York, NY.

[9] M. G. Alford, A. Schmitt, K. Rajagopal and T. Schfer, Rev. Mod. Phys. **80**, 1455 (2008) [arXiv:0709.4635 [hep-ph]].

[10] K. Fukushima and T. Hatsuda, Rept. Prog. Phys. **74**, 014001 (2011) [arXiv:1005.4814 [hep-ph]].

[11] M. G. Alford, K. Rajagopal and F. Wilczek, Nucl. Phys. B **537**, 443 (1999) [hep-ph/9804403].

[12] Z. G. Wang, S. L. Wan and W. M. Yang, hep-ph/0508302.

[13] M. Huang, P. -f. Zhuang and W. -q. Chao, Chin. Phys. Lett. **19**, 644 (2002) [hep-ph/0110046].

¡UNUSED¿

[14] M. Huang, P. -f. Zhuang and W. -q. Chao, Phys. Rev. D **65**, 076012 (2002) [hep-ph/0112124].

[15] M. Huang, Int. J. Mod. Phys. E **14**, 675 (2005) [hep-ph/0409167].

[16] F. Wilczek, In *Shifman, M. (ed.) et al.: From fields to strings, vol. 1* 77-93 [hep-ph/0409168].

[17] Y. Nishida and H. Abuki, Phys. Rev. D **72**, 096004 (2005) [hep-ph/0504083].

[18] L. He and P. Zhuang, Phys. Rev. D **75**, 096003 (2007) [hep-ph/0703042].

[19] E. J. Ferrer and J. P. Keith, Phys. Rev. C **86**, 035205 (2012) [arXiv:1201.2203 [nucl-th]].

[20] J. Deng, A. Schmitt and Q. Wang, Phys. Rev. D **76**, 034013 (2007) [nucl-th/0611097].

[21] A. H. Rezaeian and H. J. Pirner, Nucl. Phys. A **779**, 197 (2006) [nucl-th/0606043]. L. He and P. Zhuang, Phys. Rev. D **76**, 056003 (2007) [arXiv:0705.1634 [hep-ph]]. G. -f. Sun, L. He and P. Zhuang, Phys. Rev. D **75**, 096004 (2007) [hep-ph/0703159]. H. Abuki, Nucl. Phys. A **791**, 117 (2007) [hep-ph/0605081]. M. Kitazawa, D. H. Rischke and I. A. Shovkovy, Phys. Lett. B **663**, 228 (2008) [arXiv:0709.2235 [hep-ph]]. H. Abuki and T. Brauner, Phys. Rev. D **78**, 125010 (2008) [arXiv:0810.0400 [hep-ph]]. J. Deng, J. -c. Wang and Q. Wang, Phys. Rev. D **78**, 034014 (2008) [arXiv:0803.4360 [hep-ph]]. D. Blaschke and D. Zablocki, Phys. Part. Nucl. **39**, 1010 (2008) [arXiv:0812.0589 [hep-ph]]. T. Brauner, Phys. Rev. D **77**, 096006 (2008) [arXiv:0803.2422 [hep-ph]]. J. O. Andersen, Nucl. Phys. A **820**, 171C (2009) [arXiv:0809.2892 [hep-ph]]. H. Guo, C. -C. Chien and Y. He, Nucl. Phys. A **823**, 83 (2009) [arXiv:0812.1782 [hep-ph]]. B. Chatterjee, H. Mishra and A. Mishra, Phys. Rev. D **79**, 014003 (2009) [arXiv:0804.1051 [hep-ph]]. T. Hatsuda, M. Tachibana, N. Yamamoto and G. Baym, Phys. Rev. Lett. **97**, 122001 (2006) [hep-ph/0605018]. N. Yamamoto, M. Tachibana, T. Hatsuda and G. Baym, Phys. Rev. D **76**, 074001 (2007) [arXiv:0704.2654 [hep-ph]]. T. Hatsuda, M. Tachibana

and N. Yamamoto, Phys. Rev. D **78**, 011501 (2008) [arXiv:0802.4143 [hep-ph]]. N. Yamamoto and T. Kanazawa, Phys. Rev. Lett. **103**, 032001 (2009) [arXiv:0902.4533 [hep-ph]]. H. Basler and M. Buballa, Phys. Rev. D **82**, 094004 (2010) [arXiv:1007.5198 [hep-ph]]. H. Abuki, G. Baym, T. Hatsuda and N. Yamamoto, Phys. Rev. D **81**, 125010 (2010) [arXiv:1003.0408 [hep-ph]]. J. -c. Wang, Q. Wang and D. H. Rischke, Phys. Lett. B **704**, 347 (2011) [arXiv:1008.4029 [nucl-th]]. J. -c. Wang, V. de la Incera, E. J. Ferrer and Q. Wang, Phys. Rev. D **84**, 065014 (2011) [arXiv:1012.3204 [nucl-th]].

[22] J. Ranninger, arXiv:1207.6911 [cond-mat.supr-con].

[23] Y. Aoki, G. Endrodi, Z. Fodor, S. D. Katz and K. K. Szabo, Nature **443**, 675 (2006) [hep-lat/0611014].

[24] C. DeTar and U. M. Heller, Eur. Phys. J. A **41**, 405 (2009) [arXiv:0905.2949 [hep-lat]].

[25] E. J. Ferrer, V. de la Incera, J. P. Keith and I. Portillo, arXiv:1405.7422 [hep-ph].

[26] R. Casalbuoni, R. Gatto, M. Mannarelli, G. Nardulli and M. Ruggieri, Phys. Lett. B **605**, 362 (2005) [Erratum-ibid. B **615**, 297 (2005)] [hep-ph/0410401]. M. Alford and Q. -h. Wang, J. Phys. G **31**, 719 (2005) [hep-ph/0501078]. K. Fukushima, Phys. Rev. D **72**, 074002 (2005) [hep-ph/0506080].

[27] P. F. Bedaque and T. Schfer, Nucl. Phys. A **697**, 802 (2002) [hep-ph/0105150]. A. Kryjevski and T. Schfer, Phys. Lett. B **606**, 52 (2005) [hep-ph/0407329]. A. Gerhold and T. Schfer, Phys. Rev. D **73**, 125022 (2006) [hep-ph/0603257].

[28] M. G. Alford, J. A. Bowers and K. Rajagopal, Phys. Rev. D **63**, 074016 (2001) [hep-ph/0008208]. I. Giannakis and H. -C. Ren, Phys. Lett. B **611**, 137 (2005) [hep-ph/0412015]. R. Casalbuoni, R. Gatto, N. Ippolito, G. Nardulli and M. Ruggieri, Phys. Lett. B **627**, 89 (2005) [Erratum-ibid. B **634**, 565 (2006)] [hep-ph/0507247]. M. Ciminale, G. Nardulli, M. Ruggieri and R. Gatto, Phys. Lett. B **636**, 317 (2006) [hep-

ph/0602180]. K. Rajagopal and R. Sharma, Phys. Rev. D **74**, 094019 (2006) [hep-ph/0605316].

[29] E. J. Ferrer and V. de la Incera, Phys. Rev. Lett. **97**, 122301 (2006) [hep-ph/0604136].

Curriculum Vitae

Jason Keith received his Bachelor of Science degree in Physics from the University of Texas at El Paso in 2012. During this degree he was awarded for research excellence by the College Office of Undergraduate Initiatives (COURI) and the Department of Physics, inducted into the Sigma Pi Sigma physics honor society, and engaged in research with Dr. Ferrer and the high-energy theory group at UTEP which lead to a publication (Phys.Rev.C82:065802,2010). As an undergraduate he also had many opportunities to go to conferences and present research, spent one summer at Virginia Tech for an REU, and worked on campus as a TA. Continuing with his education he began working toward an M.S. degree in physics which will be completed in Spring of 2014 pending the approval of this Thesis.